

Lattice dynamics and related diffusion properties of intermetallics: II. Ni_3Sb

This article has been downloaded from IOPscience. Please scroll down to see the full text article.

1997 J. Phys.: Condens. Matter 9 10283

(<http://iopscience.iop.org/0953-8984/9/46/025>)

View [the table of contents for this issue](#), or go to the [journal homepage](#) for more

Download details:

IP Address: 171.66.16.209

The article was downloaded on 14/05/2010 at 11:07

Please note that [terms and conditions apply](#).

Lattice dynamics and related diffusion properties of intermetallics: II. Ni₃Sb

O G Randl†‡, W Petry§, G Vogl‡, W Bührer|| and B Hennion¶

† Institut Laue–Langevin, BP 156X, 38042 Grenoble Cédex 9, France

‡ Institut für Materialphysik der Universität Wien, 1090 Wien, Austria

§ Physikdepartment E13, TU München, 85748 Garching, Germany

|| Labor für Neutronenstreuung, PSI, 5232 Villigen PSI, Switzerland

¶ Laboratoire Léon Brillouin, CEN Saclay, 91191 Gif-sur-Yvette, France

Received 11 July 1997

Abstract. The phonon dispersion of the intermetallic Ni_{72.5}Si_{27.5} has been studied by inelastic neutron scattering in its high-temperature phase of DO₃ structure, stable above 530 °C. The dispersion has been examined at a temperature of 600 °C; some selected branches were also studied at 530 °C (i.e. very close to the phase transition) and at 900 °C. In general, the phonons are very strongly damped and some branches have not been found at all. For transverse phonons with [ξξ0] propagation, the frequency does not change as a function of the temperature, but the widths become larger towards higher temperatures. The migration enthalpy and several other thermodynamic quantities have been calculated from the densities of states. The anomalous behaviour of the alloy is related to high vacancy densities.

1. Introduction

Intermetallic alloys (also referred to as intermetallics) are characterized by strong bonding forces acting between their constituents. These bonds are responsible for their high degree of order, but also their strength and brittleness. Surprisingly, the atomic mobilities of the constituents can be very high, which has remained unexplained for a long time. The mechanism of diffusion in some of these alloys has been investigated directly by quasielastic neutron scattering (QNS) (NiSb: Vogl *et al* 1993; Ni₃Sb: Vogl *et al* (1996)) and by Mössbauer spectroscopy (Fe₃Si and FeAl: Sepiol and Vogl 1993, Vogl and Sepiol 1994, Feldwisch *et al* 1995).

Ni₃Sb is a particularly interesting case. The DO₃ high-temperature phase (space group: *Fm* $\bar{3}$ *m*) forms martensitically at a temperature of 530 °C (Ni_{72.5}Sb_{27.5}) from a mixture of two room-temperature phases. The Ni diffusivity in this alloy is extremely high, higher than any self-diffusivities hitherto observed in a metallic system (Heumann and Stüer 1966, Wever *et al* 1989). Quasielastic neutron scattering studies (Vogl *et al* 1996) have shown that the Ni diffusion mechanism is very simple—diffusion takes place via nearest-neighbour jumps. This mechanism, which had also been found in stoichiometric Fe₃Si by Sepiol and Vogl (1993), cannot account for extraordinarily high diffusivities. From a comparison of high-temperature x-ray densities and macroscopic densities of quenched samples Heumann and Stüer (1966) concluded that high amounts of vacancies existed. Their guess was recently confirmed by neutron diffraction studies (Randl *et al* 1996): being confined to the Ni sites, the vacancies are ordered, which makes them observable by diffraction.

There is no doubt that the high vacancy densities play an important role in favouring the Ni mobility, but there might be another reason for the high diffusivities: the DO₃ structure is very similar to the monoatomic bcc structure, in which Petry *et al* (1991) have been able to establish a link between fast diffusion and anomalies in the phonon dispersion of bcc metals ('phonon-enhanced diffusion'). The present work tries to answer the question of whether such an enhancement is operative in Ni₃Sb. Irrespective of the answer to this question, the measurements presented herein allow us to study the effects of high vacancy densities on the phonon dispersion.

The primitive unit cell of the DO₃ structure is shown in figure 1. There is one sublattice populated exclusively by Sb atoms (referred to as β)—the remaining three sites per primitive unit cell are occupied by Ni atoms. Ni₃Sb being stable only off stoichiometry, the relative excess of Sb atoms is compensated by vacancies on the Ni sites (Randl *et al* 1996). Two of the three Ni sites are symmetrically equivalent: we distinguish α (four Ni and four Sb nearest neighbours) and γ sites (all the nearest neighbours are Ni atoms).

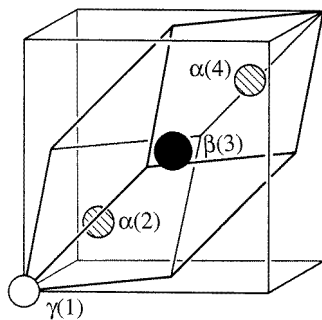


Figure 1. The primitive unit cell of the DO₃ structure. There are four atoms on three symmetrically different sites in the primitive unit cell: in the case of perfect order, the α and γ sites are occupied by Ni, the β sites by Sb atoms. The indexing of these sites ($i = 1, \dots, 4$) is noted in brackets.

There is only a little published experimental information on phonon dispersions of systems with DO₃ order. The most intensely studied system is Fe₃Al (Kentzinger *et al* 1996 and references therein). There have also been measurements on Cu–Zn–Al (Zolliker 1992) and a study of selected phonon branches of Cu–Al–Ni (Morii and Iizumi 1985) and Au–Cu–Zn (Mori *et al* 1975) near the martensitic phase transition. In a first paper (Randl *et al* 1995) we presented an extensive study of the phonon dispersion of Fe₃Si as a function of temperature and alloy composition.

2. Samples and experimental details

Polycrystalline Ni₃Sb rods were prepared using an induction furnace. The materials used were Ni sponge (purity: 99.998%) from Advent Research Materials and Sb lumps (purity 99.995%) from Goodfellow Metals. The Sb lumps were crushed in an agate mortar. An Al₂O₃ crucible was filled with both ingredients under argon atmosphere, and was held in the furnace by means of a graphite crucible, designed to reduce temperature inhomogeneities and to decrease the residual oxygen pressure. As antimony possesses a high vapour pressure, the alloying was carried out under an atmosphere of 400 Torr of high-purity argon (6 N). The alloy rods had a diameter of 8 mm and a length of approximately 100 mm. More details on the alloying technique can be found elsewhere (Randl 1994).

As already mentioned above, Ni₃Sb is a high-temperature phase (see figure 2), formed in a transition of martensitic character. A single crystal of the DO₃ phase is destroyed when cooled down to room temperature. Therefore, in a first series of measurements the single crystals were grown *in situ* (i.e. on the spectrometer), using a special *in situ* crystal growth furnace, as described in a paper by Flottman *et al* (1987). Typically, the crystal mosaicity was of one degree. Later on, it turned out that the single crystals could be 'recycled', i.e. they re-appeared when heated beyond the phase transition, even though the single crystal had been transformed into a polycrystalline lump of the low-temperature structure by cooling. Thus, the crystals could be used several times without great changes in quality (the mosaicity typically increased by 0.2 degrees per cycle), which sensibly facilitated the measurements (no need to grow *in situ*). In most cases perfect orientational memory has been observed, i.e. the crystal recovered exactly the same orientation, but in a few cases a change of orientation was found.

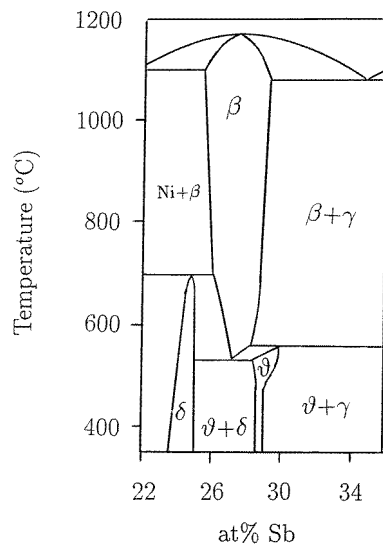


Figure 2. Phase diagram of the Ni-Sb system, from Heinrich *et al* (1978).

Due to the fact that the crystals were grown from the melt, only single crystals of a composition corresponding to the maximum in the solidus (i.e. Ni_{72.5}Sb_{27.5}) could be obtained. Therefore, we have not been able to study the dependence of the phonon dispersion on the alloy composition. The chemical composition of the samples was checked by microprobe analysis and found to agree very well with the nominal value (72.5 at.% Ni).

In most cases, the orientation of the single crystals was such that the rod axis was parallel to [001]. In order to measure phonons with a propagation vector along [111], the samples were tilted inside the furnace by means of a special Nb sample holder. Thus, the whole dispersion could be studied using the same crystal. The fine adjustment of the crystal in the measuring plane was done by means of two goniometers on which the furnace was tilted.

During the measurements, the orientation and condition of the single crystals was checked by measuring the intensity of the different Bragg peaks on the three-axis spectrometer.

Inelastic neutron scattering measurements were performed on the three-axis spectrometer IN5 of the Paul-Scherrer-Institut, but mostly on 1-T of the Orphée reactor of the Laboratoire Léon Brillouin (LLB). Most of the scans were performed with constant final wave-vector $k_f = 2.66 \text{ \AA}^{-1}$, using a PG(002) monochromator and analyser as well as a graphite filter to suppress $\lambda/2$ contributions. No additional horizontal collimation was used; the effective horizontal collimation was $25'/30'/50'/50'$.

All the measurements were performed with the sample mounted in an ILL standard resistance furnace (Ibel 1994). The vacua obtained were in the order of 10^{-6} mbar or better. The sample temperature was measured with two independent thermocouples. The nominal temperature was stable to $\pm 2^\circ\text{C}$, the absolute error at high temperatures is estimated to be less than 10°C .

The measurements have been carried out at several different temperatures: we tried to measure the whole dispersion at 600°C , and several selected branches (especially the phonons belonging to $T_{[\xi-\xi 0]}[\xi\xi 0]$, a candidate for softening) were measured at 530°C (i.e. extremely close to the phase transition) and at 900°C . Higher temperatures were avoided, as we had found out (by weighing) that the antimony loss due to evaporation became measurable above 950°C .

3. Conventions

We use a Born–von Kármán (BvK) model in the axial approximation in order to parametrize the phonon dispersion. The notation used for the different phonon branches and force constants is the same as that of Randl *et al* (1995).

4. Results

4.1. Phonon dispersion

The measurements on Ni_3Sb turned out to be much more difficult than the series performed on Fe_3Si before. First, the high incoherent scattering cross section, which had made Ni_3Sb an ideal candidate for QNS studies, is a great drawback for coherent inelastic measurements, as it gives rise to a strong background and, therefore, decreases the signal-to-noise ratio. Secondly, different from Fe_3Si , the minority component atom (Sb) is much heavier than the atoms of the majority component (Ni). The resulting decrease in energy, especially of the highest optical branch, makes a separation of the different branches more difficult. Finally, it turned out that most phonons in Ni_3Sb are extremely damped (i.e. broadened). An example is given in figures 3 and 4, where the $T_{[\xi-\xi 0]}[\xi\xi 0]$ branches of Ni_3Sb and Fe_3Si (at similar temperatures) are shown.

The combination of these three effects made it impossible to unambiguously identify phonons of energies beyond 5 THz. Furthermore, although we tried several times, on different spectrometers, using big crystals, we were not able to measure discrete phonons of the longitudinal Λ_1 branches (see figure 5). The rather incomplete dispersion at 600°C is shown in figure 6, together with the BvK model fits.

4.2. Born–von Kármán (BvK) fits

As mentioned above, we use a BvK model with longitudinal and transversal springs (L–T model), which means that there are two force constants per atom pair and nearest neighbour.

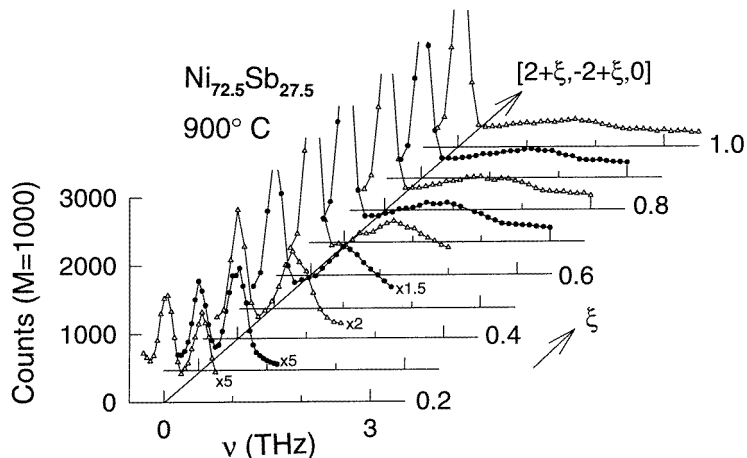


Figure 3. The $T_{[\xi-\xi 0][\xi \xi 0]}$ branch of $Ni_{72.5}Sb_{27.5}$ at $900^\circ C$.

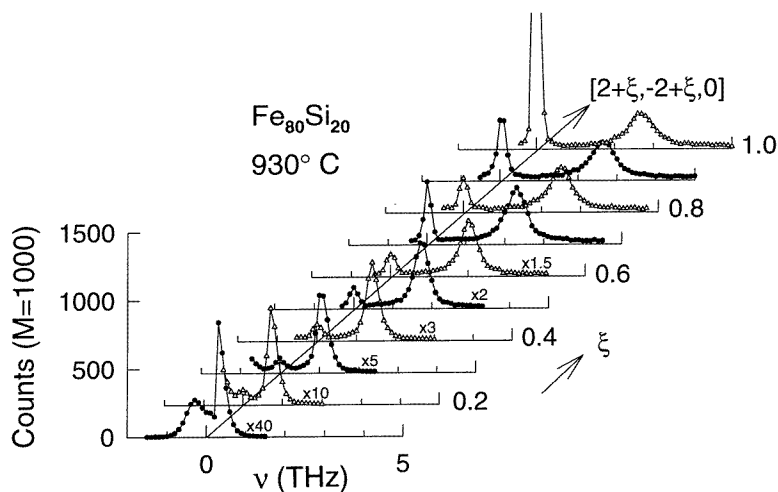


Figure 4. The $T_{[\xi-\xi 0][\xi \xi 0]}$ branch of $Fe_{80}Si_{20}$ at $930^\circ C$.

As discussed in our previous paper (Randl *et al* 1995), the limitation to an L-T model is reasonable.

The number of shells that have to be taken into account is found by trial: the set of fit parameters is increased until the fit quality does not improve any more. We found that in the case of DO_3 order a set of 16 force constants (corresponding to interactions between up to the fourth-nearest neighbours) was sufficient.

Of course, the order of the alloy should be taken into account when the BvK fit is performed. From our diffraction results (Randl *et al* 1996), we expect 12% of the Ni sites to be vacant. However, as no appropriate theory is available, the vacancies have not been taken into consideration in the BvK fit.

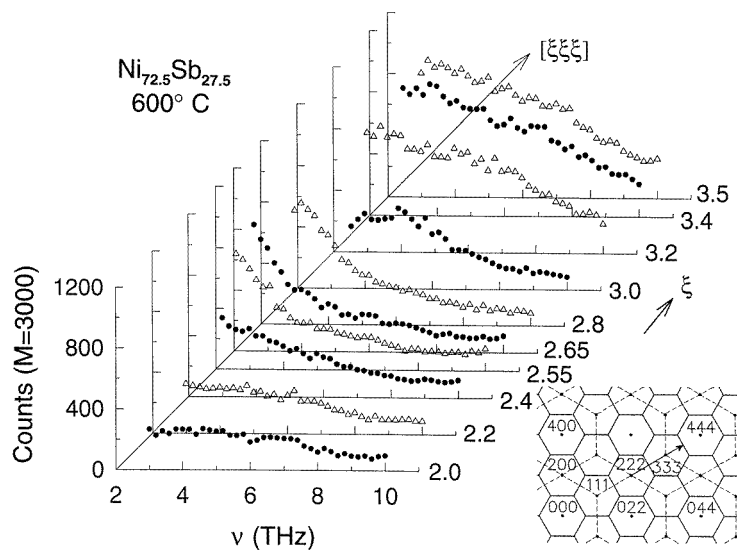


Figure 5. Intensities measured along the $[\xi\xi\xi]$ direction in reciprocal space. The absence of clearly defined phonons is obvious. Note that the dynamical structure factor is such that at each Q value at least one phonon branch should be visible.

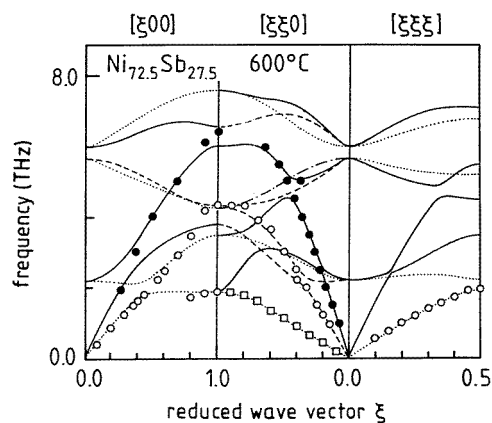


Figure 6. Dispersion of $\text{Ni}_{72.5}\text{Sb}_{27.5}$ at 600°C . The lines correspond to a BvK fit.

One crucial difficulty concerning the BvK fits consists in the correct attribution of measured phonons to the theoretically expected phonon branches; we followed the same procedure as described earlier (Randl *et al* 1995).

Table 1 lists the force constants obtained for $\text{Ni}_{72.5}\text{Sb}_{27.5}$ at 600°C . At the other temperatures only a few branches have been measured; therefore, no BvK fit was carried out.

A BvK fit is useful for parametrizing dispersion relations, but it has no deep physical signification. However, some conclusions may be drawn from table 1. Obviously, the interaction between Ni–Sb pairs $L_1(23)$ is much stronger than the Ni–Ni interaction $L_1(12)$, whereas in Fe_3Si the Fe–Si and Fe–Fe interactions are of similar strength: so to speak,

Table 1. BvK force constants (in $N\ m^{-1}$) for $Ni_{72.5}Sb_{27.5}$ at $600\ ^\circ C$. The values for $Fe_{75}Si_{25}$ at $930\ ^\circ C$ are given for the sake of comparison.

	$Ni_{72.5}Sb_{27.5}$ $600\ ^\circ C$	$Fe_{75}Si_{25}$ $930\ ^\circ C$
$L_1(12)$	13.0(4)	46.7(8)
$T_1(12)$	-4.8(1)	-1.9(2)
$L_1(23)$	64.1(7.3)	43.0(9)
$T_1(23)$	-4.9(2)	-4.2(4)
$L_2(13)$	7.6(3)	12.3(3)
$T_2(13)$	-0.2(2)	0.1(3)
$L_2(24)$	15.4(4)	14.9(4)
$T_2(24)$	-0.8(2)	-3.1(3)
$L_3(11)$	5.3(5)	7.4(4)
$T_3(11)$	-0.1(1)	-3.7(4)
$L_3(22)$	1.3(4)	0.6(4)
$T_3(22)$	-0.1(1)	1.8(3)
$L_4(33)$	24.5(1.7)	0.1(4)
$T_4(33)$	-0.5(2)	-0.8(3)
$L_4(12)$	-1.0(1)	-1.5(3)
$L_4(12)$	-1.0(1)	1.5(3)

Ni_3Sb merits the label ‘intermetallic alloy’ to a higher degree. This fact is also reflected in the phase diagram: Ni_3Sb is separated from pure Ni by a two-phase region, whereas Fe_3Si gradually disorders into a solid solution of Si in Fe. The force constants belonging to the second shell are similar in both systems. Please note the strong Sb–Sb interaction $L_3(33)$, which has no equivalent in Fe_3Si .

4.3. Phonon widths

As we have already seen above, the phonons of Ni_3Sb are very strongly damped. Is there a strong dependence on temperature, especially close to the martensitic phase transition? Figure 7 shows the effect of temperature on both frequency and width of phonons of the $T_{[\xi-\xi 0]}[\xi\xi 0]$ branch. Within the precision of our measurements there is hardly any temperature effect on the frequency of the phonons. There is no change of width between 600 and $530\ ^\circ C$, although the latter is very close to the phase transition. However, the phonons at $900\ ^\circ C$ are more strongly damped.

4.4. Derived quantities

From the BvK force constants we can calculate several important quantities. First, it is possible to derive the elastic constants. Their analytical expression (in terms of the force constants) is derived using the long-wavelength approximation. The expressions being quite lengthy, we refer the reader to the derivation given by Randl (1995). The following elastic constants are found: $C_{11} = 25.3$; $C_{44} = 8.7$; $C_{12} = 5.3$; $C' = 3.2$ (all in $10^{10}\ N\ m^{-2}$). Note that these constants can be regarded as reliable because they are determined from the initial slopes of the acoustic phonon branches, which have been measured, and not by the missing high-energy phonons. Ni_3Sb being a high-temperature phase, no literature data on the elastic constants are available, but efforts are being undertaken to perform high-temperature ultrasonic measurements in order to confirm these values.

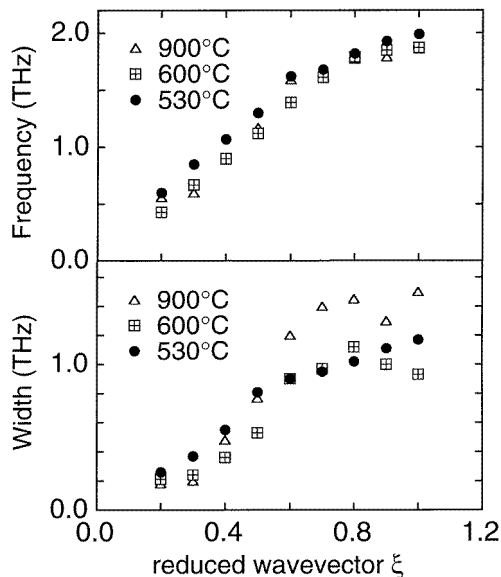


Figure 7. Temperature dependence of the phonon frequencies and widths (damped oscillator) for the $T_{[\xi-\xi_0][\xi\xi_0]}$ branch of $\text{Ni}_{72.5}\text{Sb}_{27.5}$.

Secondly, the normalized density of states $Z(\nu)$ can be obtained from the dispersion relation $\nu_S(\mathbf{q})$ by an integration over the Brillouin zone (Gilat–Raubenheimer method). Of course, $Z(\nu)$ is not reliable at higher frequencies (where hardly any phonons have been found), but we are above all interested in the thermodynamical quantities that can be derived from $Z(\nu)$ and which are determined by the measured low-frequency modes. The corresponding part of $Z(\nu)$ is reliable.

As shown in our previous paper (Randl *et al* 1995), it is possible to calculate the mean square displacement and the Debye temperature as well as the migration enthalpy from the density of states. We find the following values for $\text{Ni}_{72.5}\text{Sb}_{27.5}$ at 600 °C: $\langle u_\alpha^2 \rangle = 3.2 \times 10^{-2} \text{ \AA}^2$, $\Theta_D = 232.1 \text{ K}$, and $H_M = 0.27 \text{ eV}$. The latter value is distinctly lower than in Fe_3Si , which reflects the fact that diffusion in Ni_3Sb is faster than in Fe_3Si .

5. Discussion

Is the anomalously fast Ni diffusion in Ni_3Sb linked to ‘phonon enhancement’? In spite of the incompleteness of our data, some conclusions can be drawn. First of all, we have not observed any softening of a particular phonon group, even very close to the martensitic phase transformation. This is in agreement with results on CuZnAl (Zolliker 1992) and fcc Co (Strauss *et al* 1996). Unlike the high-temperature bcc phases of some pure metals, Ni_3Sb does not show dynamical precursor effects near the phase transformation. Their absence underlines the first-order character of the martensitic phase transition.

The most astonishing feature in the phonon dispersion of Ni_3Sb are the badly defined, smeared-out phonon groups. As the effect becomes stronger at high temperatures (and not when approaching the phase transition), we conclude that it is not related to precursors of the low-temperature phase. Therefore, the model of ‘phonon enhancement’ appears to be inappropriate to explain fast diffusion in Ni_3Sb . Diffusion is undoubtedly favoured by the

low migration barrier, which is also reflected in the acoustic phonons of low frequency and the relatively weak Ni–Ni interaction. However, the migration enthalpy alone cannot account for the extraordinarily high Ni mobilities that have been observed. However, it should be noted in this context that our approach to calculate H_M is only a first approximation. Originally, the equation for H_M was derived for elementary metals. The underlying concept of harmonic vibrations may be questionable in a system exhibiting such broad phonon distributions.

What are the effects of high vacancy densities on the dispersion? We think that the strong phonon broadening is due to the high defect density. The latter leads to structural heterogeneities or vibrational anharmonicities, even at 600 °C. As the temperature is raised, the atoms experience greater elongations from their equilibrium positions. They probe the perturbations of the lattice potential due to defects, the concentration of which is temperature independent (Randl *et al* 1996). Obviously, one would not expect stronger broadening near the phase transition. Although this model is able to qualitatively explain the strong anharmonicities and their temperature behaviour, it is still purely speculative: to our knowledge, the influence of a great number of (ordered) vacancies on the dynamics of a lattice has not been studied yet theoretically.

6. Conclusion

As a conclusion, let us come back to the comparison of the two systems we have examined, Fe₃Si and Ni₃Sb. Both alloys adopt DO₃ structure, but there are striking differences, due to the strength of interaction between the alloy constituents. In Fe₃Si, the Fe–Si interaction is more or less equivalent to its Fe–Fe counterpart. When the Fe content is increased, Fe₃Si gradually disorders into a solid solution of Si in Fe. Ni₃Sb, however, is separated from pure Ni by a two-phase region, which is due to the Ni–Sb interaction being much stronger than the Ni–Ni interaction. Within the DO₃ phase, deviation from stoichiometry is made up by disorder (Fe₃Si) or by the creation of structural vacancies in certain sublattices (Ni₃Sb). As disorder increases in Fe₃Si, the phonon frequencies and widths change continuously, as expected for a system undergoing a phase transition of second-order type. As far as we can say, Ni₃Sb behaves differently: there are no precursor effects near the phase transformation, which underlines the first-order character of the transition. The smearing out of phonon groups increases with temperature, although the order of the alloy is not disturbed. We relate this result to the fact that the atoms are elongated more strongly and, therefore, the influence of the defects in their surrounding increases.

Acknowledgments

One of the authors (OGR) wishes to thank Wolfgang Miekeley (HMI Berlin) for the first Ni₃Sb rods and precious know-how, Andreas Heimig for his initiation in the art of crystal growth, and Jürgen Neuhaus for his introduction into phonon measurements.

Financial support by the Austrian Fonds zur Förderung der Wissenschaftlichen Forschung (FWF), contracts S5601 and S5605, is gratefully acknowledged.

References

- Feldwisch R, Sepiol B and Vogl G 1995 *Acta Metall. Mater.* **43** 2033
- Flottmann T, Petry W, Serve R and Vogl G 1987 *Nucl. Instrum. Methods A* **260** 165
- Heinrich S, Rexer H U and Schubert K 1978 *J. Less Comm. Met.* **60** 65

- Heumann T and Stüer H 1966 *Phys. Status Solidi* **15** 95
- Ibel K (ed) 1994 *Guide to Neutron Research Facilities at the ILL* (Grenoble: ILL)
- Kentzinger E, Cadeville M C, Pierron-Bohnes V, Petry W and Hennion B 1996 *J. Phys.: Condens. Matter* **8** 5535
- Morii and Iizumi 1985 *J. Phys. Soc. Japan* **54** 2948
- Petry W, Heimig A, Herzig C and Trampenau J 1991 *Defect Diffusion Forum* **75** 211
- Randl O G 1994 *Thesis* Institut für Festkörperphysik, University of Vienna, available from the authors
- 1995 *ILL Report* 95RA13T
- Randl O G, Vogl G, Kaisermayr M, Bühner W, Pannetier J and Petry W 1996 *J. Phys.: Condens. Matter* **8** 7691
- Randl O G, Vogl G, Petry W, Hennion B, Sepiol B and Nembach K 1995 *J. Phys.: Condens. Matter* **7** 5983
- Sepiol B and Vogl G 1993 *Phys. Rev. Lett.* **71** 731
- Strauss B, Frey F, Petry W, Trampenau J, Nicolaus K, Shapiro S M and Bossy J 1996 *Phys. Rev. B* **54** 6035
- Vogl G, Kaisermayr M and Randl O G 1996 *J. Phys.: Condens. Matter* **8** 4727
- Vogl G, Randl O G, Petry W and Hünecke J 1993 *J. Phys.: Condens. Matter* **5** 7215
- Vogl G and Sepiol B 1994 *Acta Metall. Mater.* **42** 3175
- Wever H, Hünecke J and Frohberg G 1989 *Z. Metallk.* **80** 389
- Zolliker M 1992 *Thesis* 9577, ETH Zürich